



Published in final edited form as:

Science. 2012 January 13; 335(6065): 229–232. doi:10.1126/science.1214448.

iRhom2 Regulation of TACE Controls TNF-Mediated Protection Against *Listeria* and Responses to LPS

David R. McIlwain^{1,2,*}, Philipp A. Lang^{1,3,*}, Thorsten Maretzky⁴, Koichi Hamada⁵, Kazuhito Ohishi⁶, Sathish Kumar Maney³, Thorsten Berger¹, Aditya Murthy⁷, Gordon Duncan¹, Haifeng C. Xu^{1,3}, Karl S. Lang^{3,8}, Dieter Häussinger³, Andrew Wakeham¹, Annick Itie-Youten¹, Rama Khokha⁷, Pamela S. Ohashi^{1,2}, Carl P. Blobel^{4,9}, and Tak W. Mak^{1,2,†}

¹Campell Family Institute for Breast Cancer Research, Ontario Cancer Institute, University Health Network (UHN), 620 University Avenue, Toronto, Ontario M5G 2C1, Canada

²Department of Medical Biophysics, University of Toronto, 1 King's Circle, Toronto, Ontario M5S 1A8, Canada

³Department of Gastroenterology, Hepatology and Infectious Diseases, University of Düsseldorf, Universitätsstrasse 1, 40225 Düsseldorf, Germany

⁴Arthritis and Tissue Degeneration Program, Hospital for Special Surgery, New York, NY 10021, USA

⁵Okada Projects at the Center for AIDS Research, Kumamoto University, 2-2-1 Honjo, Kumamoto 860-0811, Japan

⁶Department of Pathology, Graduate School of Medicine, Osaka University, 2-2 Yamada-oka, Suita, Osaka 565-0871, Japan

⁷Ontario Cancer Institute, UHN, Toronto, Ontario, M5G 2M9, Canada

⁸Institute for Immunology, University of Essen, Hufelandstrasse 55, 45147 Essen, Germany

⁹Departments of Medicine and of Physiology, Biophysics and Systems Biology, Weill Medical College of Cornell University, New York, NY 10021, USA

Abstract

Innate immune responses are vital for pathogen defense but can result in septic shock when excessive. A key mediator of septic shock is tumor necrosis factor- α (TNF α), which is shed from the plasma membrane after cleavage by the TNF α convertase (TACE). We report that the rhomboid family member iRhom2 interacted with TACE and regulated TNF α shedding. iRhom2

[†]To whom correspondence should be addressed: tmak@uhnresearch.ca.

*These authors contributed equally to this work.

Link to final version published in Science: www.sciencemag.org/content/335/6065/229

Supporting Online Material

www.sciencemag.org/cgi/content/full/VOL/ISSUE/PAGE/DC1

Materials and Methods

Figs. S1 to S8

Table S1

References (24–33)

was critical for TACE maturation and trafficking to the cell surface in hematopoietic cells. Gene-targeted iRhom2-deficient mice showed reduced serum TNF α in response to lipopolysaccharide (LPS) and could survive a lethal LPS dose. Furthermore, iRhom2-deficient mice failed to control the replication of *Listeria monocytogenes*. Our study has identified iRhom2 as a regulator of innate immunity that may be an important target for modulating sepsis and pathogen defense.

Tumor necrosis factor- α (TNF α) is both crucial for effective innate immunity and a pathologic contributor to inflammatory diseases, including sepsis and rheumatoid arthritis (1–4). How TNF α signaling is regulated, however, is still not fully understood. To identify new molecules involved in regulating TNF α signaling, we performed an unbiased cyclic packaging rescue screen (5) to isolate cDNAs conferring TNF α resistance. One such candidate was a short cDNA (iRhom2*) derived from the gene encoding iRhom2 (Rhbdf2) (fig. S1), which is a largely uncharacterized member of the rhomboid protein family (6–8). Stable overexpression of iRhom2* in L929 cells revealed its localization in the endoplasmic reticulum (ER), consistent with previous studies of iRhoms (8–10), and partial localization in the Golgi apparatus (fig. S2). iRhom2* overexpression protected L929 cells from TNF α -induced apoptosis (Fig. 1A). Experiments using the metalloproteinase inhibitor BB-2516 suggested that this TNF α resistance was the result of metalloprotease (MP)-dependent release of TNF α receptors (TNFRs) from the cell surface (Fig. 1, B and C). Because TNFR shedding is mediated by TNF α convertase (TACE) (also known as a disintegrin and MP (ADAM) 17) (11), we investigated whether iRhom2 interacts with TACE. Mature TACE is generated after processing of its prodomain in the Golgi (12, 13). By preparing cell lysates in the presence of MP inhibitors to prevent autocatalytic degradation of mature TACE (12) and by performing Concanavalin A (ConA) lectin purification, we were able to use immunoblotting to clearly distinguish immature (or pro-TACE) from the active mature form of TACE (fig. S3). Immunoprecipitation of lysates of iRhom2-overexpressing fibroblasts followed by immunoblotting revealed a physical association between tagged-iRhom2 and both pro- and mature forms of TACE, which suggested that iRhom2 and TACE are associated through multiple stages of the secretory pathway (Fig. 1D). This interaction appears specific, as no such association with other ADAM family members, including ADAM9 and ADAM15, could be detected (Fig. 1D). These data suggested that association with iRhom2 might be important for regulating TACE activity.

To investigate whether the relation between iRhom2 and TACE was physiologically relevant, we generated mice deficient for the gene that encodes iRhom2 (*iRhom2*^{-/-}) in which exons 4 to 14 of the *iRhom2* gene were deleted, which abolished expression of *iRhom2* mRNA (fig. S4). *iRhom2*^{-/-} mice are viable and fertile, show no obvious defects, have a normal life-span, and exhibit a normal immune cell distribution (table S1). Because TACE is classically known to be the enzyme responsible for production of soluble TNF α through surface shedding (14, 15), we analyzed TNF α production by macrophages. When thioglycollate-elicited peritoneal macrophages (TGEMs) were isolated from control (*iRhom2*^{+/+} or *iRhom2*^{+/-}) mice and stimulated in vitro with the Toll-like receptor (TLR) 4 ligand lipopolysaccharide (LPS), the mRNA levels of iRhom2, TACE, and TNF α were all increased (fig. S5, A to C). TACE and TNF α mRNA levels were comparably up-regulated in LPS-stimulated *iRhom2*^{-/-} TGEMs (fig. S5, B and C), but significantly less TNF α

protein was shed into mutant cell culture supernatants than into control supernatants (Fig. 2A). Consistent with a block in membrane-bound TNF α cleavage (16) in the absence of iRhom2, LPS-treated *iRhom2*^{-/-} TGEMs accumulated higher expression of membrane-bound TNF α than controls (Fig. 2B, left). Treatment with BB-2516 mimicked iRhom2 deficiency, as it increased levels of membrane-bound TNF α on LPS-stimulated wild-type (WT) TGEMs to levels observed on untreated *iRhom2*^{-/-} TGEMs (Fig. 2B, right). No difference in the secretion of other LPS-induced cytokines, such as interleukin-6 (IL-6) or IL-12, was observed (fig. S5, D and E). Although a mechanism of triggering IL-12 production involving processing of the TNF α intracellular domain has been described (17), proficient IL-12 production in *iRhom2*^{-/-} macrophages after LPS is consistent with other mouse models incapable of producing soluble TNF α (18).

TACE is also crucial for the stimulus-dependent cleavage of other substrates from the surfaces of immune cells, including L-selectin (CD62L) (11). Granulocytes and CD4⁺ T cells that were isolated from *iRhom2*^{-/-} mice and stimulated in vitro with phorbol-12-myristate-13-acetate (PMA) to activate TACE (11) showed impaired CD62L surface down-regulation compared with controls (Fig. 2C). Similarly, when WT and *iRhom2*^{-/-} B cells were stimulated with the nucleotide analog 2'(3')-O-(4-benzoyl)benzoyl adenosine 5'-triphosphate (BzATP) to induce shedding of both CD62L and CD23 (an ADAM10 substrate), only CD62L shedding was inhibited in *iRhom2*^{-/-} B cells (Fig. 2D). We also detected elevated surface expression of another TACE substrate, intercellular adhesion molecule-1 (19), on *iRhom2*^{-/-} TGEMs (fig. S5F). Taken together, these results suggest that iRhom2 is specifically required for TACE-mediated shedding of multiple surface molecules, including TNF α , from immune cell surfaces.

To determine potential mechanisms by which iRhom2 might control TACE activity, we examined the status of TACE maturation in the absence of iRhom2. Using immunoblotting, we readily detected both the inactive pro- and active mature forms of TACE in splenocytes and bone marrow-derived macrophages (BMDMs) from control mice. However, *iRhom2*^{-/-} splenocytes and BMDMs exhibited only pro-TACE expression (Fig. 2E and fig. S6A). When we analyzed the subcellular localization of hemagglutinin (HA)-tagged TACE (TACE-HA) in WT BMDMs by immunofluorescence microscopy, TACE was broadly distributed, which included prominence in the cell periphery. In contrast, TACE appeared mislocalized in *iRhom2*^{-/-} BMDMs, as it was restricted to granular vesicular compartments. (Fig. 2F and fig. S6, B and C). No discernible differences were observed in ADAM10-HA localization between WT and *iRhom2*^{-/-} BMDMs (Fig. 2F and fig. S6B). To examine if this phenotype held true for endogenous TACE, we isolated cell surface proteins from BMDMs by biotinylation and probed for endogenous TACE by immunoblotting. Consistent with our microscopy data, mature TACE was correctly localized in cell surface fractions of WT BMDMs, whereas *iRhom2*^{-/-} BMDMs exclusively expressed only minute quantities of pro-TACE at the cell surface (Fig. 2G). These data suggest that iRhom2 is critical for triggering TACE maturation and trafficking to the cell surface and may explain why iRhom2 is necessary for TACE activity in immune cells.

To examine the consequences of iRhom2-mediated regulation of TACE maturation in vivo, we injected control and *iRhom2*^{-/-} mice with LPS and determined serum TNF α levels. The

mutants showed dramatically less serum TNF α than controls (Fig. 3A), and granulocytes isolated from these animals exhibited decreased LPS-stimulated down-regulation of CD62L (Fig. 3B and fig. S7A). A well-known model of TNF α -mediated septic shock and liver damage involves the combined injection of LPS and D-galactosamine (GalN) (4). When we injected control and *iRhom2*^{-/-} mice with LPS and GalN, serum TNF α was reduced in the mutants, whereas IL-6, IL-12, and interferon- γ (IFN γ) levels were comparable with those in controls (fig. S7B). Examination of liver histology 6 hours after injection showed that 87% of LPS- and GalN-treated control mice showed disrupted liver architecture, compared with only 35% of LPS- and GalN-treated *iRhom2*^{-/-} mice (Fig. 3C). In terms of lethality, whereas most LPS- and GalN-treated control mice died within 24 hours, most LPS- and GalN-treated *iRhom2*^{-/-} mice survived beyond the 48 hours of the experiment (Fig. 3D). However, treatment of control and *iRhom2*^{-/-} mice with recombinant TNF α and GalN led to similar rates of death (Fig. 3E and fig. S7, C and D). Thus, although in vivo responses to exogenous TNF α are normal in *iRhom2*^{-/-} mice, endogenous production of soluble TNF α is impaired, such that these mutants are resistant to LPS lethality.

TNF α and TNFRI are crucial for defense against bacterial infections (4, 16, 20, 21). To determine whether *iRhom2* is required for TNF α -mediated antibacterial activity, we infected TGEMs from untreated control and *iRhom2*^{-/-} mice with the intracellular bacterium, *L. monocytogenes*. Little TNF α was detected in the supernatants of infected *iRhom2*^{-/-} TGEM cultures (Fig. 4A). When control and *iRhom2*^{-/-} mice were infected with *L. monocytogenes*, serum levels of IL-6, IL-12, and IFN γ were comparable (fig. S8A), and no differences in granulocyte infiltration were observed in spleen or liver (fig. S8B). Although granuloma formation and intracellular *L. monocytogenes* were detected in liver tissues of both control and *iRhom2*^{-/-} mice (Fig. 4B), more granulomas were present in infected *iRhom2*^{-/-} liver than in the control (Fig. 4C). In addition, *L. monocytogenes* titers in spleen, liver, kidney, and brain were all significantly higher in *iRhom2*^{-/-} mice than in controls 4 days after infection (Fig. 4D). As a result, *iRhom2*^{-/-} mice rapidly succumbed to the infection (Fig. 4E), a pattern that held true even at bacterial doses that were nonlethal for control mice (Fig. 4F). Thus, *iRhom2* is critical for defense against *L. monocytogenes*.

Our data support a role of *iRhom2* as an essential factor for the activity and trafficking of TACE in hematopoietic cells and are supported by the results presented in the accompanying manuscript by Adrain *et al.* (22). Mice with a myeloid cell-specific deletion in TACE, are similar to *iRhom2*^{-/-} mice in that both are resistant to LPS-induced septic shock and defective in generating soluble TNF α (23). Unlike what we observed in the *iRhom2*^{-/-} mice, TACE-deficient (*Adam17*^{-/-}) mice often die perinatally (11). These differences may be the result of cell-, or context-specific effects of *iRhom2* function. The inhibition of *iRhom2* may represent a potential new therapeutic approach for treating TNF α -mediated diseases.

Supplementary Material

Refer to Web version on PubMed Central for supplementary material.

Acknowledgments

The authors thank S. Le Gall, S. McCracken, A. Elia, E. Arpaia, and J. Height for experimental assistance and M. Saunders for scientific editing. The data reported in this manuscript are tabulated in the main paper and in the Supporting Online Material. P.A.L. was supported by the Sofja Kovalevskaja Award 2010 of the Alexander von Humboldt Foundation and the Strategic Research Fund of the Heinrich Heine University. K.S.L. was funded by the Sofja Kovalevskaja Award 2008 of the Alexander von Humboldt Foundation; Deutsche Forschungsgemeinschaft grant LA1419/3-1; and the Molecules of Infection Center, Manchot Graduate School (Jürgen Manchot Foundation). This study was supported by the Collaborative Research Center 575 (SFB575: Experimental Hepatology; Coordinator: D.H.). C.P.B. was supported by NIH GM64750, and T.M. by the Emerald Foundation. K.O. was supported in part by the Naito Foundation; the Mochida Memorial Foundation for Medical and Pharmaceutical Research; the Senri Life Science Foundation; and the Ministry of Education, Culture, Sports, Science and Technology of Japan. T.W.M., D.R.M., and K.O. have filed U.S. Patent Application No: 61/426,396 regarding the use of iRhom2 for regulating innate immunity. This work was generously supported by funding from the Canadian Institutes of Health Research and the Terry Fox Foundation.

References and Notes

1. Scott DL, Kingsley GH. Tumor necrosis factor inhibitors for rheumatoid arthritis. *N Engl J Med*. 2006; 355:704.10.1056/NEJMct055183 [PubMed: 16914706]
2. Palladino MA, Bahjat FR, Theodorakis EA, Moldawer LL. Anti-TNF-alpha therapies: The next generation. *Nat Rev Drug Discov*. 2003; 2:736.10.1038/nrd1175 [PubMed: 12951580]
3. Feldmann M. Development of anti-TNF therapy for rheumatoid arthritis. *Nat Rev Immunol*. 2002; 2:364.10.1038/nri802 [PubMed: 12033742]
4. Pfeffer K, et al. Mice deficient for the 55 kd tumor necrosis factor receptor are resistant to endotoxic shock, yet succumb to L. monocytogenes infection. *Cell*. 1993; 73:457.10.1016/0092-8674(93)90134-C [PubMed: 8387893]
5. Bhattacharya D, Logue EC, Bakkour S, DeGregori J, Sha WC. Identification of gene function by cyclical packaging rescue of retroviral cDNA libraries. *Proc Natl Acad Sci USA*. 2002; 99:8838.10.1073/pnas.132274799 [PubMed: 12084928]
6. Koonin EV, et al. The rhomboids: A nearly ubiquitous family of intramembrane serine proteases that probably evolved by multiple ancient horizontal gene transfers. *Genome Biol*. 2003; 4:R19.10.1186/gb-2003-4-3-r19 [PubMed: 12620104]
7. Lemberg MK, Freeman M. Functional and evolutionary implications of enhanced genomic analysis of rhomboid intramembrane proteases. *Genome Res*. 2007; 17:1634.10.1101/gr.6425307 [PubMed: 17938163]
8. Zettl M, Adrain C, Strisovsky K, Lastun V, Freeman M. Rhomboid family pseudoproteases use the ER quality control machinery to regulate intercellular signaling. *Cell*. 2011; 145:79.10.1016/j.cell.2011.02.047 [PubMed: 21439629]
9. Zou H, et al. Human rhomboid family-1 gene RHBDF1 participates in GPCR-mediated transactivation of EGFR growth signals in head and neck squamous cancer cells. *FASEB J*. 2009; 23:425.10.1096/fj.08-112771 [PubMed: 18832597]
10. Nakagawa T, et al. Characterization of a human rhomboid homolog, p100hRho/RHBDF1, which interacts with TGF-alpha family ligands. *Dev Dyn*. 2005; 233:1315.10.1002/dvdy.20450 [PubMed: 15965977]
11. Peschon JJ, et al. An essential role for ectodomain shedding in mammalian development. *Science*. 1998; 282:1281.10.1126/science.282.5392.1281 [PubMed: 9812885]
12. Schlöndorff J, Becherer JD, Blobel CP. Intracellular maturation and localization of the tumour necrosis factor alpha convertase (TACE). *Biochem J*. 2000; 347:131.10.1042/0264-6021:3470131 [PubMed: 10727411]
13. Reiss K, Saftig P. The "a disintegrin and metalloprotease" (ADAM) family of sheddases: Physiological and cellular functions. *Semin Cell Dev Biol*. 2009; 20:126.10.1016/j.semcdb.2008.11.002 [PubMed: 19049889]
14. Black RA, et al. A metalloproteinase disintegrin that releases tumour-necrosis factor-alpha from cells. *Nature*. 1997; 385:729.10.1038/385729a0 [PubMed: 9034190]

15. Moss ML, et al. Cloning of a disintegrin metalloproteinase that processes precursor tumour-necrosis factor-alpha. *Nature*. 1997; 385:733.10.1038/385733a0 [PubMed: 9034191]
16. Alexopoulou L, et al. Transmembrane TNF protects mutant mice against intracellular bacterial infections, chronic inflammation and autoimmunity. *Eur J Immunol*. 2006; 36:2768.10.1002/eji.200635921 [PubMed: 16983719]
17. Friedmann E, et al. SPPL2a and SPPL2b promote intramembrane proteolysis of TNFalpha in activated dendritic cells to trigger IL-12 production. *Nat Cell Biol*. 2006; 8:843.10.1038/ncb1440 [PubMed: 16829952]
18. Torres D, et al. Membrane tumor necrosis factor confers partial protection to *Listeria* infection. *Am J Pathol*. 2005; 167:1677.10.1016/S0002-9440(10)61250-3 [PubMed: 16314479]
19. Tsakadze NL, et al. Tumor necrosis factor-alpha-converting enzyme (TACE/ADAM-17) mediates the ectodomain cleavage of intercellular adhesion molecule-1 (ICAM-1). *J Biol Chem*. 2006; 281:3157.10.1074/jbc.M510797200 [PubMed: 16332693]
20. Pasparakis M, Alexopoulou L, Episkopou V, Kollias G. Immune and inflammatory responses in TNF alpha-deficient mice: A critical requirement for TNF alpha in the formation of primary B cell follicles, follicular dendritic cell networks and germinal centers, and in the maturation of the humoral immune response. *J Exp Med*. 1996; 184:1397.10.1084/jem.184.4.1397 [PubMed: 8879212]
21. Rothe J, et al. Mice lacking the tumour necrosis factor receptor 1 are resistant to TNF-mediated toxicity but highly susceptible to infection by *Listeria monocytogenes*. *Nature*. 1993; 364:798.10.1038/364798a0 [PubMed: 8395024]
22. Adrain C, Zettl M, Christova Y, Taylor N, Freeman M. Tumor necrosis factor signaling requires iRhom2 to promote trafficking and activation of TACE. *Science*. 2012; 335:6065.
23. Horiuchi K, et al. Cutting edge: TNF-alpha-converting enzyme (TACE/ADAM17) inactivation in mouse myeloid cells prevents lethality from endotoxin shock. *J Immunol*. 2007; 179:2686. [PubMed: 17709479]
24. Horiuchi K, et al. Substrate selectivity of epidermal growth factor-receptor ligand sheddases and their regulation by phorbol esters and calcium influx. *Mol Biol Cell*. 2007; 18:176.10.1091/mbc.E06-01-0014 [PubMed: 17079736]
25. McIlwain DR, et al. Smg1 is required for embryogenesis and regulates diverse genes via alternative splicing coupled to nonsense-mediated mRNA decay. *Proc Natl Acad Sci USA*. 2010; 107:12186.10.1073/pnas.1007336107 [PubMed: 20566848]
26. Weskamp G, Krätzschmar J, Reid MS, Blobel CP. MDC9, a widely expressed cellular disintegrin containing cytoplasmic SH3 ligand domains. *J Cell Biol*. 1996; 132:717.10.1083/jcb.132.4.717 [PubMed: 8647900]
27. Lum L, Reid MS, Blobel CP. Intracellular maturation of the mouse metalloprotease disintegrin MDC15. *J Biol Chem*. 1998; 273:26236.10.1074/jbc.273.40.26236 [PubMed: 9748307]
28. Lang PA, et al. Tissue macrophages suppress viral replication and prevent severe immunopathology in an interferon-I-dependent manner in mice. *Hepatology*. 2010; 52:25.10.1002/hep.23640 [PubMed: 20578253]
29. Lang PA, et al. Aggravation of viral hepatitis by platelet-derived serotonin. *Nat Med*. 2008; 14:756.10.1038/nm1780 [PubMed: 18516052]
30. Lang PA, et al. Hematopoietic cell-derived interferon controls viral replication and virus-induced disease. *Blood*. 2009; 113:1045.10.1182/blood-2007-10-117861 [PubMed: 18971424]
31. Navarini AA, et al. Increased susceptibility to bacterial superinfection as a consequence of innate antiviral responses. *Proc Natl Acad Sci USA*. 2006; 103:15535.10.1073/pnas.0607325103 [PubMed: 17030789]
32. Sauer B, Henderson N. Site-specific DNA recombination in mammalian cells by the Cre recombinase of bacteriophage P1. *Proc Natl Acad Sci USA*. 1988; 85:5166.10.1073/pnas.85.14.5166 [PubMed: 2839833]
33. Bernsel A, Viklund H, Hennerdal A, Elofsson A. TOPCONS: Consensus prediction of membrane protein topology. *Nucleic Acids Res*. 2009; 37:W465. Web Server issue. 10.1093/nar/gkp363 [PubMed: 19429891]

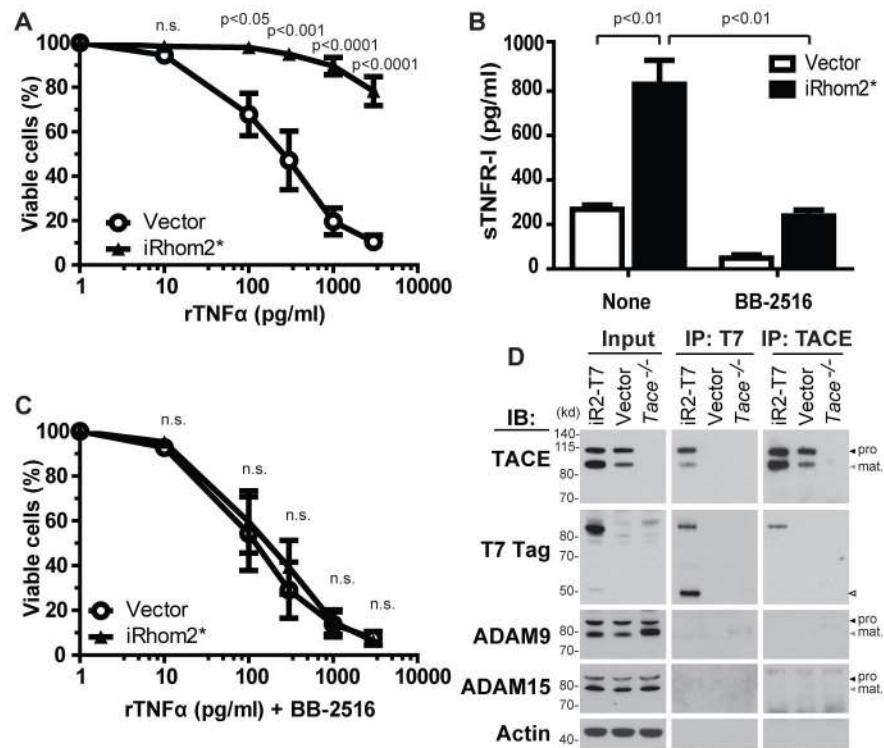
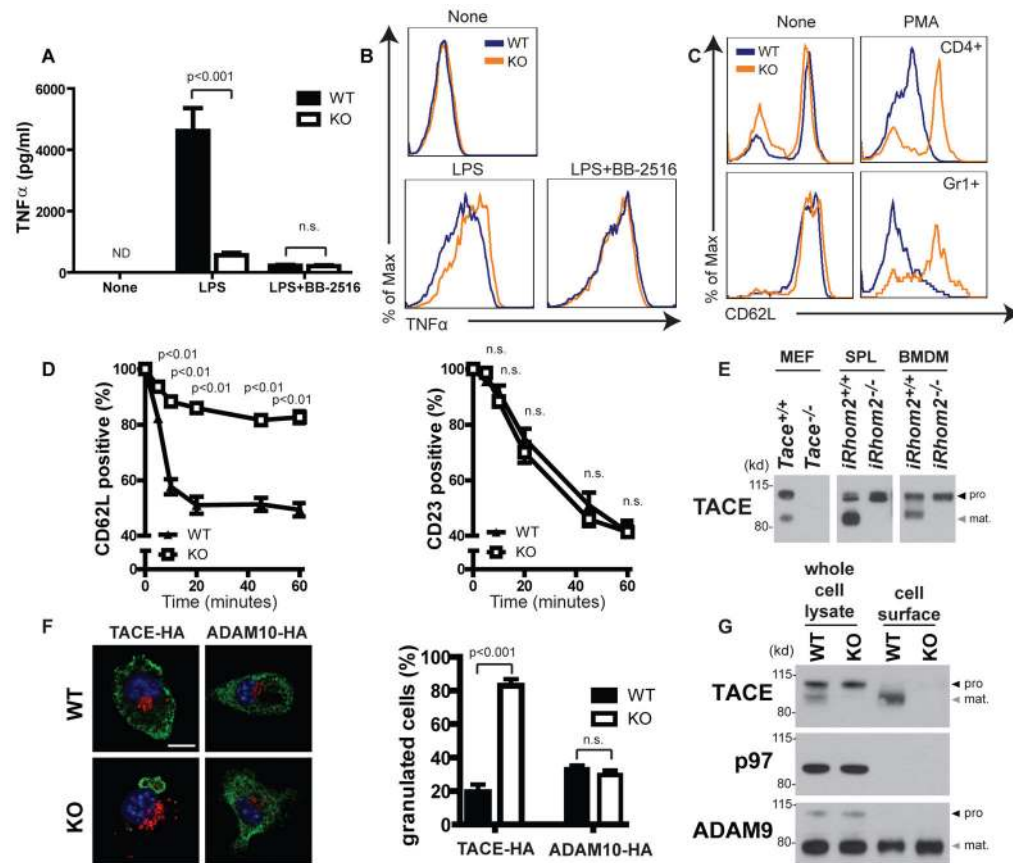


Fig. 1. iRhom2 confers resistance to TNF α in a MP-dependent manner and interacts with TACE. (A) L929 cells stably overexpressing iRhom2* or control vector were treated with recombinant TNF α (rTNF α) at the indicated concentrations, and percent viability was determined by Annexin-7AAD exclusion (means \pm SEM; $n = 4$ experiments). (B) Untreated cells from (A) were cultured with or without metalloproteinase inhibitor BB-2516 (20 μ M) for 24 hours. Soluble TNFR1 in the culture supernatant was measured by enzyme-linked immunosorbent assay (ELISA) (means \pm SEM; $n = 3$ experiments). (C) Cells from (A) were treated for 24 hours with TNF α at the indicated concentrations plus 20 μ M BB-2516, and viability was assessed as in (A) (means \pm SEM; $n = 4$ experiments). (D) WT immortalized mouse embryonic fibroblasts (MEFs) stably overexpressing T7-tagged iRhom2 (iR2-T7) or control vector and *Adam17*^{-/-} (*TACE*^{-/-}) MEFs (negative control) were immunoprecipitated (IP) by using antibodies against T7 or TACE followed by immunoblotting (IB) to detect T7 or TACE. ADAM9 and ADAM15 were specificity controls; actin, loading control. Black arrowheads indicate immature pro-forms, whereas gray arrowheads indicate mature forms, of TACE and other ADAMs (for all figures). Empty arrowhead is likely a processed form of iRhom2. ConA purification was used to enhance detection of TACE in input lanes (unpurified input appears in fig. S3). Results are representative of three trials.

**Fig. 2.**

iRhom2 deficiency reduces TACE activity in vitro. (**A** and **B**) WT and *iRhom2*^{-/-} TGEMs were stimulated in vitro with 1 μ g/ml LPS, with or without 20 μ M BB-2516. (**A**) TNF α in culture supernatants was determined by ELISA after 24 hours of treatment (means \pm SEM of triplicates). (**B**) Membrane-bound TNF α was assayed by flow cytometry after 3 hours of treatment. Results are representative of three trials. (**C**) Isolated WT and *iRhom2*^{-/-} total splenocytes were stimulated in vitro with 25 ng/ml PMA for 3 hours, and CD62L expression on CD4⁺ T cells and Gr1⁺ granulocytes was determined by flow cytometry. Results are representative of three trials. (**D**) WT and *iRhom2*^{-/-} total splenocytes were stimulated with 2 mM BzATP for the indicated times, and surface levels of CD62L and CD23 (ADAM10 substrate) on B220⁺CD3⁻ B cells were determined by flow cytometry (means \pm SEM; n = 3 mice per group). (**E**) ConA-purified lysates of control and *iRhom2*^{-/-} splenocytes (SPL) or BMDMs were immunoblotted to detect pro- (black arrowhead) and mature (gray arrowhead) TACE. *Adam17*^{-/-} (*TACE*^{-/-}) MEFs, negative control. Additional controls appear in fig. S6A. Results are representative of three trials. (**F**) (Top) Control and *iRhom2*^{-/-} BMDMs were transfected with vectors expressing TACE-HA or ADAM10-HA (green), stimulated with LPS, and visualized by confocal immunofluorescence microscopy. Giantin (red) and 4', 6'-diamidino-2-phenylindole (DAPI) stain (blue). Scale bar, 10 μ m. (Bottom) Percentages of control and *iRhom2*^{-/-} BMDMs that exhibited granulated vesicular appearance of TACE or ADAM10 localization (means \pm SEM; n = 4 to 6 experiments). (**G**) (Top) Immunoblot to detect pro- (black arrowhead) and mature (gray arrowhead) TACE in whole-cell lysates and

purified cell surface fractions of control and *iRhom2*^{-/-} BMDMs. (Middle) P97, intracellular protein (negative control). (Bottom) Pro- (black arrowhead) and mature (gray arrowhead) ADAM9 (positive control). Results are representative of three trials.

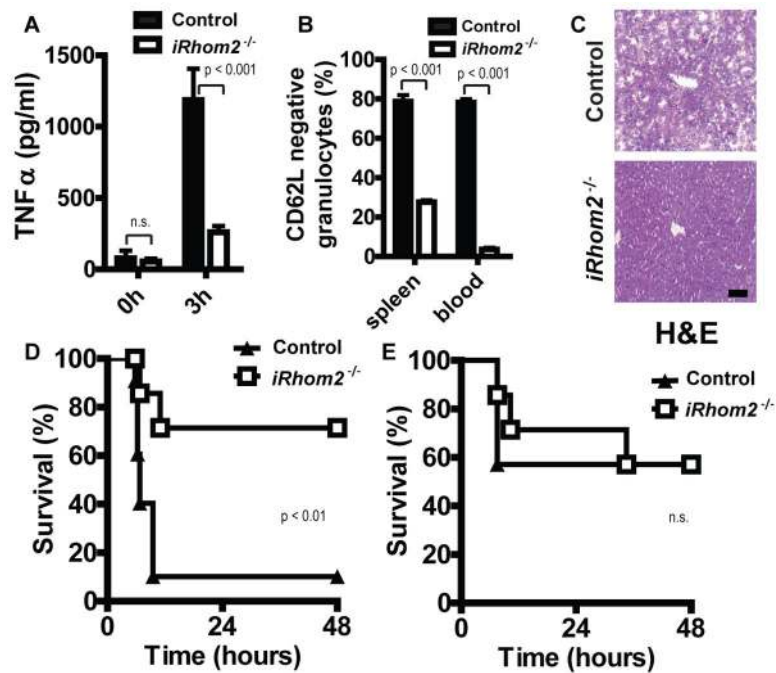


Fig. 3.

iRhom2 deficiency prevents LPS-induced liver pathology by inhibiting TNF α shedding. (A and B) Control and *iRhom2*^{-/-} mice ($n = 4$ per group) were intravenously injected with 0.14 mg per mouse LPS O111:B4. Serum TNF α (A) and CD62L⁻Gr1⁺CD11b⁺ cells in spleen and blood (B) were measured 3 hours after injection by ELISA or flow cytometry, respectively. (C) Control ($n = 7$) and *iRhom2*^{-/-} ($n = 8$) mice were intraperitoneally injected with 10 mg GalN, followed 20 min later by intravenous injection of 0.05 mg LPS O111:B4. Livers were snap-frozen 6 hours after injection and sections stained with hematoxylin and eosin (H&E). Control panel is representative for six out of seven samples. *iRhom2*^{-/-} panel is representative for five out of eight samples. Scale bar, 100 μ m. (D) Control and *iRhom2*^{-/-} mice ($n = 10$ to 11 per group) were injected with GalN and LPS as for (C), and survival was monitored for 48 hours. (E) Control and *iRhom2*^{-/-} mice ($n = 7$ per group) were intraperitoneally injected with 10 mg GalN, followed 20 min later by intravenous injection of 0.15 μ g rTNF α . Survival was monitored for 48 hours.

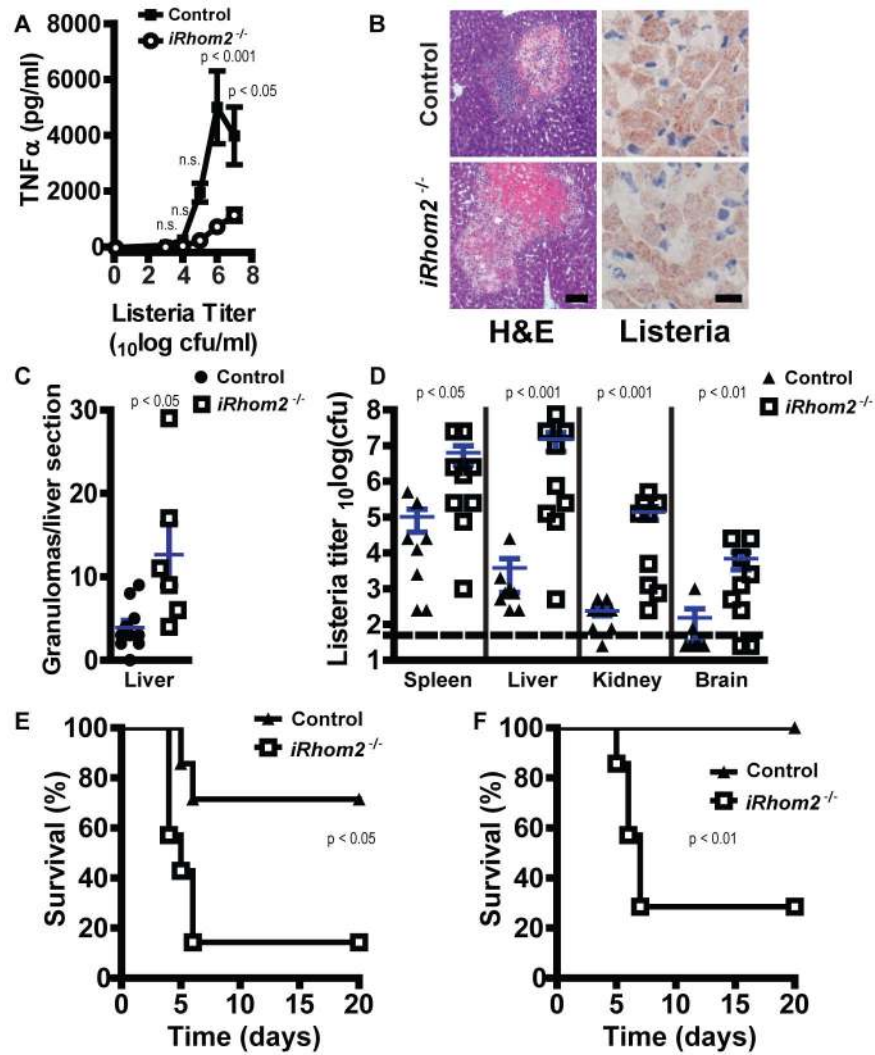


Fig. 4. *iRhom2* is crucial for control of *L. monocytogenes*. **(A)** TGEMs (10^5) isolated from control or *iRhom2*^{-/-} mice ($n = 5$ to 8 per group) were exposed to the indicated titers of *L. monocytogenes* for 24 hours. TNF α in culture supernatants was determined by ELISA (means \pm SEM). **(B)** Control and *iRhom2*^{-/-} mice ($n = 6$ to 10 per group) were infected with 10^4 colony-forming units (cfu) *L. monocytogenes*. Livers were isolated on day 4 after infection, sectioned, and stained with H&E (left) or with antibody against *Listeria* (right). Scale bars: left, 100 μ m; right, 20 μ m. **(C)** Granulomas were counted in F4/80-stained liver sections (not shown) from the mice in (B). Data points are granulomas or liver of individual mice. Blue lines, means \pm SEM ($n = 6$ to 10 per group). **(D)** Control and *iRhom2*^{-/-} mice ($n = 8$ to 9 mice per group) were infected with 10^5 cfu *L. monocytogenes*, and bacterial titers were determined in spleen, liver, kidney, and brain on day 4 after infection. Data points are titers of individual mice. Dashed line, limit of detection. Blue lines, means \pm SEM. **(E)** and **(F)** Control and *iRhom2*^{-/-} mice ($n = 7$ per group) were infected with 5×10^4 cfu (E) or 5×10^3 cfu (F) *L. monocytogenes*, and mouse survival was monitored for 20 days.